Impact of polymer-modified gold nanoparticles on brain endothelial cells: exclusion of endoplasmic reticulum stress as a potential risk factor.

Laura Anspach[1], Ronald E. Unger[1], Matthew I. Gibson[2], Harm-Anton Klok[3], C. James Kirkpatrick[1], Christian Freese*[1]

Address: [1]REPAIR-lab, Institute of Pathology, University Medical Center of the Johannes Gutenberg University Mainz and European Institute of Excellence on Tissue Engineering and Regenerative Medicine, Mainz, Germany; [2]University of Warwick, Department of Chemistry, Coventry, CV4 7AL, United Kingdom; [3] École Polytechnique Fédérale de Lausanne (EPFL), Institut des Matériaux and Institut des Sciences et Ingénierie Chimiques, Laboratoire des Polymères, Bâtiment MXD, Station 12, CH-1015 Lausanne, Switzerland.

*Corresponding author: Christian Freese, Langenbeckstr. 1, 55131 Mainz, Germany; Phone: +49-6131-17-3925, Email: freesec@uni-mainz.de

Keywords

Unfolded Protein Response, cell stress, tight junction proteins, BiP, blood-brain barrier

Abstract

A library of polymer-coated gold nanoparticles (AuNPs) differing in size and surface modifications was examined for uptake and induction of cellular stress responses in the endoplasmic reticulum (ER stress) in human brain endothelial cells (hCMEC/D3). ER stress is known to affect the physiology of endothelial cells (ECs) and may lead to inflammation or apoptosis. Thus, even if applied at non-cytotoxic concentrations ER stress caused by nanoparticles should be prevented to reduce the risk of vascular diseases and negative effects on the integrity of barriers (e.g. blood-brain barrier). We exposed hCMEC/D3 to twelve different AuNPs (three sizes: 18, 35, and 65 nm, four surface-modifications) for various times and evaluated their effects on cytotoxicity, proinflammatory mediators, barrier functions and factors involved in ER stress. We demonstrated a time-dependent uptake of all AuNPs and no cytotoxicity for up to 72h of exposure. Exposure to certain AuNPs resulted in a time-dependent increase in the proinflammatory markers IL-8, MCP-1, sVCAM, sICAM. However, none of the AuNPs induced an increase in expression of the chaperones and stress sensor proteins BiP and GRP94, respectively, or the transcription factors ATF4 and ATF6. Furthermore, no upregulation of the UPR stress sensor receptor PERK, no active splicing product of the transcription factor XBP1 and no upregulation of the transcription factor CHOP were detectable. In conclusion, the results of the present study indicate that effects of different-sized gold nanoparticles modified with various polymers were not related to the induction of ER stress in brain microvascular endothelial cells or led to apoptosis.

Abbreviations

IRE1a: inositol-requiring enzyme 1 a, UPR unfolded protein response, BiP: immunoglobulin heavy-chain-binding protein, xbp1: X-box binding protein 1, PERK: protein kinase RNA-like ER kinase, ATF: activating transcription factor, CHOP: CCAAT-enhancer-binding protein homologous protein, GRP94: glucose-regulated protein 94, ZO-1: *zonula occludens*-1.

Introduction

Detailed studies of the interactions of nanoparticles with healthy cells *in vitro* are necessary to ensure nanoparticle safety, especially if nanoparticles are targeted for use in biomedical applications such as radiation therapy, imaging (contrast agents), and regenerative medicine or as drug delivery systems. Gold nanoparticles (AuNPs) are chemically inert and have been shown to be biocompatible if the nanoparticles are not ultrasmall or do not contain stabilizing agents such as cetyltrimethylammonium bromide (CTAB) or citrate (Connor et al. 2005; Uboldi et al. 2009; Freese et al. 2012b; Pan et al. 2007). However, there is still a need to examine each newly synthesized particle to exclude toxicity due to the absence of sufficient data to permit the classification of nanoparticles as ‘toxic’ or ‘non-toxic’, based solely on their physico-chemical characteristics. Even if AuNPs do not affect cell viability, nanoparticles have been shown to induce various cellular responses, including the secretion of proinflammatory mediators in dendritic cells (Villiers et al. 2010), or reactive oxygen species (ROS) production in brain tissue and liver of mice (Shrivastava et al. 2014).

Surface modification with polymers can decrease the toxic effects of AuNPs (Alkilany A. M. et al. 2009). In addition, the modification of surfaces of AuNPs with various polymers can change their uptake properties in human dermal microvascular

endothelial cells (Freese et al. 2012a) and influence the amount of AuNPs that are internalized by endothelial cells from different locations of the body. Therefore, it may be possible to regulate targeting of AuNPs based on surface modifications and size (Freese et al. 2013).

The interaction of AuNPs with brain microvascular endothelial cells is of great interest, since brain endothelial cells form a complex and tight barrier between the blood and brain tissue, the blood-brain barrier (BBB). Any impact on brain endothelial cells that consequently leads to a disruption of the BBB will influence endothelial cell ability to protect the brain from toxic substances. One of the cellular mechanisms that may impact the integrity of endothelial cells is ER stress. ER stress may be responsible for a decreased expression of tight junction proteins in primary human retinal endothelial cells which has been shown to result in increased permeability (Adachi et al. 2012).

In general, ER stress is known to affect the function of endothelial cells and is characterized by the accumulation of unfolded and misfolded proteins in the endoplasmic reticulum. This leads to an activation of an ER stress signaling pathway, called the Unfolded Protein Response (UPR) which counteracts the stress situation. The first response of the cell is the re-establishment of homeostasis (Walter und Ron 2011; Ron und Walter 2007) by up-regulation of chaperone expression such as BiP and GRP94 (Schröder und Kaufman 2005). On the other hand, prolonged ER stress and ongoing activation of the UPR initiate apoptosis of cells (Tabas und Ron 2011). In addition, UPR plays a central role in many diseases such as diabetes and cancer (Walter und Ron 2011; Lin et al. 2008; Li et al. 2011) and a key role in various brain-related disorders such as Alzheimer’s disease, Parkinson's disease and cerebral ischemia (Fonseca, Ana Catarina R G et al. 2013;

Xin et al. 2014; Roussel et al. 2013; Reinhardt et al. 2014). Since endothelial cells play a central role in the homeostasis of tissues and organs, the healing processes and the maintenance of barriers (brain, eye, testis), it is essential that ER stress in endothelial cells caused by nanoparticles, especially those that are being considered for medical applications is prevented.

Initial studies have shown that the treatment of primary endothelial cells with silica nanoparticles can result in the induction of ER stress (Tsai et al. 2011; Christen und Fent 2012). In addition, AuNPs have been shown to lead to ER stress in human chronic myelogenous leukemia cells (Tsai et al. 2011). To the best of our knowledge, the effect of AuNPs in inducing ER stress has not been systematically investigated in endothelial cells. Thus, we have examined a library of 12 polymer-modified AuNPs with different sizes (18, 35, 65 nm), for their uptake in cultured human brain endothelial cells (hCMEC/D3), evaluated their cytotoxic activity and examined their effects on the expression of proinflammatory mediators and tight junction proteins. In addition, different ER stress-related factors were examined to determine if there were correlations with uptake and internalization, toxicity, proinflammatory marker expression or membrane integrity.

Methods

Gold nanoparticles

The gold nanoparticles were synthesized and characterized as previously described. In addition to that also the role of solution conditions on nanoparticle aggregation was discussed (Gibson et al. 2011; Freese et al. 2012a). Importantly, we demonstrated that in the ECBM MV cell culture medium (PromoCell) supplemented with 15 % fetal calf serum, all of the nanoparticles were well dispersed. The AuNPs

studied had sizes of 18 nm, 35 nm and 65 nm and were modified with different polymers (glucosamine, hydroxypropylamine, taurine, (poly)ethylenglycol) as described previously (Gibson et al. 2009; Gibson et al. 2011; Freese et al. 2013).

Cell culture

The immortalized human cerebral microvascular endothelial cell line, hCMEC/D3 was provided by Pierre-Olivier Couraud (Department of Cell Biology, Institute Cochin, Paris, France) and characterized as described previously (Weksler et al. 2005). hCMEC/D3 were maintained on fibronectin-coated culture dishes in ECBM MV cell culture medium (PromoCell) supplemented with 15 % fetal calf serum, 2.5 ng / mL basal fibroblast growth factor, 10 µg / mL sodium heparin (all Sigma-Aldrich), penicillin (100 U/mL) and streptomycin (100 µg/mL) (Gibco). The cells were sub-cultivated twice a week.

Nanoparticle treatment and microscopy

For uptake studies cells were seeded onto fibronectin-coated LabTek chamber slides (Nunc) and treated with 100 µg / mL gold nanoparticles for 24 hours. Afterwards, cells were washed and fixed in 3.7 % paraformaldehyde for 15 minutes. After permeabilization with 0.2% TritonX-100, cells were stained first with mouse anti-human CD31 antibody (DakoCytomation) and then the corresponding secondary antibody (goat anti-mouse Alexa Fluor 546; Molecular Probes) at room temperature for 1 hour each. Nuclei were counterstained with Hoechst 33342 dye (Sigma-Aldrich). The LabTek chamber slides were embedded with GelMount (Biomeda) and analyzed via light/fluorescence microscopy (Olympus IX71 with Delta Vision system, Applied Precision, USA).

For analysing the uptake of AuNPs by transmission electron microscopy cells were seeded onto fibronectin-coated Thermanox coverslips (Nunc, Roskilde, Denmark), treated with 18 nm-sized Au-NPs (10 µg / mL) as described above and then fixed with cacodylate-buffered glutaraldehyde (Serva) (pH 7.2) for 20 minutes. This was followed by a fixation step in 1% (w/v) osmium tetroxide for 2 hours and dehydration in ethanol. Cells were transferred through propylene oxide. Afterwards the samples were embedded in agar-100 resin (PLANO, Germany) and polymerized at 60°C for 48 hours. Ultrathin sections were cut with an ultramicrotome (Leica Microsystems, Germany), placed onto copper grids and stained with 1% (w/v) uranyl acetate in alcoholic solution and lead citrate. Ultrastructural analysis was performed with a transmission electron microscope, EM 410 (Philips; Eindhoven, Netherlands).

Cell viability assessment

Cells were seeded on 96-well plates (coated with fibronectin) and incubated with various concentrations of nanoparticles. Cells were then washed and cell viability was determined using the CellTiter 96 AQueous non-radioactive assay (Promega) as recommended by the manufacturer.

Quantification of internalized gold nanoparticles by ICP-AES

Internalized gold nanoparticles were quantified as described previously (Freese et al. 2012a). Briefly, after reaching confluence cells cultured on fibronectin-coated 24-well plates were exposed to AuNPs (10 µg / mL). After 24 hours of treatment cells were washed, detached by trypsin/EDTA (Gibco) solution and transferred after the addition of 0.9 mL PBS to tubes. 0.15 mL of aqua regia was added and incubated overnight. Samples were then further diluted to 5mL using MilliQ water to give a total sample volume of 5 mL. These samples were then analyzed (3X) for total gold

content by inductively coupled plasma atomic emission spectroscopy (ICP-AES) and concentrations were determined using a gold standard (Fluka Analytical). The concentration of solubilized gold and the mass of the NPs was used to calculate the number of particles. The cell number of each well was used to determine the number of particles per cell.

Determination of ER stress mediators

Treatment and cell harvesting

hCMEC/D3 were cultured on 48-well plates (TPP) until confluent and subsequently treated with various concentrations of nanoparticles. As a positive control for ER stress hCMEC/D3 were incubated with 2 µg / mL tunicamycin (Sigma) for 24 hours. After treatment and washing, cells from 3 wells were combined in RLT buffer and 1% mercapthoethanol (Qiagen) and stored at -80°C until RNA isolation.

RNA-isolation and cDNA synthesis

RNA was isolated using the RNeasy Midi Kit (Qiagen) as described by the manufacturer. The amount of RNA in each sample was measured with the NanoDrop ND1000 spectrophotometer. 300-500 ng RNA were used for the reverse transcription polymerase chain reaction according to a standard protocol using Omniscript RT kit (Qiagen), random primers (Microsynth) and RNase inhibitor (Promega GmbH).

Real-time PCR

For quantitative real-time PCR 3.75 ng cDNA were amplified using 12.5 µl of QuantiTectTM SYBR® Green PCR Master Mix and 100 nM of each primer per reaction. Quantitative real-time PCR was performed in triplicate with the 7300 Real-

time PCR System (Applied Biosystems) using the following cycler program: 95°C, 15 min; denaturation step: 94°C; 15 s; annealing step: 60°C 30 s; elongation step: 72°C 35 s; dissociation: 95°C 15 s; 60°C 1 min; 95°C 15 s, and 40 cycles were performed in total. Ribosomal protein L13a (RPL13A) was used as an endogenous control to calculate ΔΔCt. The following primers were used:

Table 1

Polymerase chain reaction

10 ng cDNA were amplified by polymerase chain reaction (PCR) with specific primer pairs (1 µM each), and a master mix containing 14.875 µl RNAse-free water, 2.5 µl 10-fold buffer, 0.5 µl 2' deoxyribonucleotides (dNTP) mix, and 0.125 µl Taq DNA polymerase (all Qiagen). PCR was performed using PCR System 9700 cycler (Applied Biosystems), 35 cycles and the following cycler program: 94°C, 2 min; 94°C, 0.5 min; 60°C, 0.5 min; 72°C, 0.5 min; 72°C, 10 min. PCR products were separated by gel electrophoresis in a 3 % agarose gel including 0.02 % ethidium bromide and 1 % Tris/Borate/EDTA buffer. The primers used have been synthesized by Microsynth:

Xbp1 u/s: for: 5'-CTGGAACAGCAAGTGGTAGA-3', rev: 5'-CTGGGTCCTTCTGGGTAGAC-3' (Shang 2005).

Enzyme-linked immunosorbent assay (ELISA)

After exposure to the nanoparticles the supernatants of the cells were diluted in the appropriate assay diluent and analyzed via ELISA (DuoSet, R&D Systems) for secreted soluble proinflammatory mediators as recommended by the manufacturer.

Data analysis

All experiments were done in triplicate and repeated as indicated. Data were analyzed with GraphPad Prism version 5.04 (GraphPad Software, San Diego California USA, www.graphpad.com).

Results

The AuNP library consisting of nanoparticles with sizes of 18, 35 and 65 nm each sequentially modified with four different coatings (glucosamine, hydroxypropylamine, taurine, poly(ethylenglycol) were screened for their effects on human brain endothelial cells (hCMEC/D3). These coatings were chosen to provide a range of surface chemistries which also give stable particles. The glucosamine, hydroxypropylamine and poly(ethyleneglycol) units are all hydrophilic coatings, but present different surface functionalities – e..g the PEG unit is well know protein - resistant, non-immunogenic polymer which cannot donate hydrogen bonds. However, the hydroxypropylamine and glucosamine can donate and accept hydrogen bonds, changing the interfacial properties. Glucosamine can also (potentially) engage with receptors and transporters on cell surfaces. The nanoparticles have been reported in a previous study using electron microscopy, light scattering and UV-Vis, confirming them to all be colloidal stable in the conditions employed.Biocompatibility was determined after exposure to different concentrations of the nanoparticles (10, 50, 100, 250 µg / mL) and at four different exposure times (4h, 24h, 48h, 72h). None of the AuNPs had any detectable effect on cell viability as determined by the measurement of the metabolic activity of the cells (see Supplementary Material Figure 1). In addition, the uptake behavior of the various AuNPs in hCMEC/D3 after 4 and 24 hours was examined. In Figure 1 A-D,

representative images of the internalization of 35 nm gold nanoparticles in brain endothelial cells are shown. The images demonstrate that depending on the modification of the AuNPs the nanoparticles were internalized in varying amounts. Light microscopy was used to identify agglomerates of internalized AuNPs. After 24 hours the AuNPs were present in the perinuclear region of the cell and transmission electron microscopy confirmed the results seen by light microscopy (Figure 1 F - I). The detailed TEM images demonstrated that AuNPs were located in vesicles (Figure 1 F' – I') but were neither freely dispersed in the cytoplasm, nor located in mitochondria or the cell nucleus. The amount of internalized AuNPs was quantified by inductively coupled plasma and atomic emission spectroscopy (ICP-AES). Briefly, after exposure and washing the cells (containing AuNPs) were digested with Aqua Regia and the total gold concentration determined. This was then converted to particles, using the TEM diameters of the gold particles, assuming a density of 19.3 $g.cm^{-3}$. This was then corrected to the cell density. This method enables us to rule out effects due to the higher volume (and hence gold atoms) of larger particles compared to smaller. The results presented in Figure 1 E show that all sizes of nanoparticles were internalized, but in different amounts. The 18 nm nanoparticles were internalized in a higher amount compared to the nanoparticles with a mean diameter of 35 nm or 65 nm. Interestingly, the uptake behavior of the 35 nm-sized hydroxypropylamine-coated AuNP was different from those of the nanoparticles with sizes of 18 nm or 65 nm highlighting the delicate balance between size and surface chemistry.

Since AuNPs were internalized in various amounts by brain endothelial cells but did not cause any cytotoxic effect, physiological functions of brain endothelial cells were examined. Cells exposed to the various AuNPs were examined to evaluate changes

in the secretion pattern of proinflammatory mediators. Interestingly, a time-dependent exposure effect on the secretion of inflammatory mediators could be observed for some but not all of the AuNPs. 4 hours of exposure to the AuNPs did not result in changes to the secretion of IL-8, MCP-1, sVCAM and sICAM (data not shown). However, after 24 hours all sizes of glucosamine-coated gold nanoparticles as well as the 35 nm hydroxypropylamine-coated nanoparticles showed an increased secretion of these cytokines compared to the untreated control (Figure 2). Moreover, a major increase in the secretion of the proinflammatory mediators was detected after increasing the incubation period to 48 and 72 hours. Decreasing the AuNP concentration lead to a decreased secretion of IL-8, IL-6 and MCP-1 (see Supplementary Material Figure 2). In summary, changes to the secretion pattern of proinflammatory mediators occurred with certain nanoparticles indicating that certain physico-chemical properties (surface modification and size) could have an impact on the physiology of brain endothelial cells while others did not. However, none of the nanoparticles induced levels of changes in proinflammatory mediator expression as achieved by the treatment of cells with the positive control, TNFα.

In addition to the effects of modified AuNPs on cell viability, uptake and secretion of proinflammatory cytokines, a further physiological function of blood-brain barrier endothelial cells, namely the presence of tight junctions, was examined after exposure to the AuNPs. In Figure 3 the expression of tight junction proteins after treatment with AuNPs is shown. The expression of occludin and ZO-1 decreased in all treated cells although not significantly. However, a significant decrease in the expression of ZO-1 was observed on cells exposed to 65 nm hydroxypropylamine-coated AuNPs. The expression of claudin-5 was less affected in cells exposed to the nanoparticles and the changes were not significant when compared to the control

cells. In summary, the expression of the tight junction proteins investigated decreased in varying amounts. A correlation of nanoparticle size or surface modification and a decrease in the expression of TJ proteins was not obvious. The larger sized NPs appeared to have a tendency towards changing tight junction protein expression, although a significant difference could not be detected.

ER stress responses were examined to determine whether these were responsible for the altered expression of tight junction proteins and the induction of secretion of proinflammatory mediators after exposure to the nanoparticles. Cells exposed to various concentrations of AuNPs were analyzed for spliced XBP1 mRNA. Figure 4 shows the results of cells examined for the spliced variant of XBP1 mRNA after treatment with AuNPs for 4 hours. In Figure 4A both the spliced and unspliced variant of XBP1 were detected. The spliced variant was observed at very low amounts even after an exposure to 150 µg / mL AuNPs, compared to the positive control, treated with tunicamycin (Figure 4 A'; Supplementary Material Figure 3 B). Real-time PCR was performed to detect the amount of spliced XBP1 in cells that were treated with 150 µg / mL AuNPs (Figure 4B). No changes in the splicing of XBP1 were observed, indicating no activation of UPR after 4 hours of AuNP exposure. In contrast, cells exposed to 18 nm AuNPs showed a decreased amount of spliced XBP1 mRNA. In addition, no increased amount of XBP1s was detected by real-time PCR in cells that were treated with AuNPs for 24 hours (see Supplementary Material Figure 3 A).

The expression patterns of further UPR mediators were examined to investigate if these were responsible for the effect of various AuNPs on ER stress in hCMEC/D3. In Figure 5, the results demonstrated that the expression of the chaperones BiP and Grp94 was not altered after treatment with various AuNPs for 4 and 24 hours. In

contrast, the treatment with tunicamycin, the positive control for UPR activation, resulted in a 14.3-fold and 13.1-fold upregulation of BiP or Grp94, respectively. Even after a prolonged exposure to nanoparticles for up to 72h, the expression of BiP was not induced (see Supplementary Material Figure 4). In addition, the expression of the transcription factor ATF4, which regulates the gene expression of UPR target genes, was also not induced by treatment with AuNPs, compared to the treatment with tunicamycin. In contrast, the expression of ATF4 after exposure to the 65 nm AuNPs coated with glucosamine (65-gluc) or hydroxypropylamine (65-hyd) for 4 hours was slightly decreased (0.6-fold) compared to the untreated control. In addition, the expression patterns of the UPR factors, IRE1α, PERK and ATF6 were analyzed. No changes were observed in the expression of PERK and ATF6. However, IRE1α expression was slightly induced after 24 hours, although a short term exposure to the NPs did not lead to an upregulation. Differences in the upregulation after 24 hours of exposure to the AuNPs were detectable. However, no correlation between the surface modification or size of the nanoparticles and the upregulation of IRE1α could be demonstrated. Finally, studies were performed to determine if the exposure of cells to AuNPs resulted in an induction of apoptosis. Nanoparticle-treated cells were examined for the induction of CHOP expression, an early mediator of ongoing apoptosis, after different exposure times. As shown in Figure 6, none of AuNPs tested induced a change in the expression of CHOP after 4 hours of treatment. Even after prolonged exposure (72 hours) the expression of CHOP did not change significantly, although a slight increase of CHOP expression after 72 hours could be shown for the medium-sized taurine-coated AuNPs (35-taurine; 1.7-fold). In summary, the AuNPs evaluated in these studies were biocompatible and non-toxic, the particles exhibited differences in their internalization by hCMEC/D3, and some of

the particles induced the expression of proinflammatory cytokines. However, none of the particles induced either the expression of prominent ER stress markers or led to an ongoing apoptosis.

Discussion

The use of AuNPs for biomedical applications is justified by their physico-chemical characteristics and biocompatibility, in particular when coated with certain polymers (Boisselier und Astruc 2009; Wilkins et al. 2015; Phillips et al. 2014). However, even if a direct toxicity of AuNPs is minimal, further studies have to be carried out prior to using these particles for medical applications to ensure that complex non-toxic interactions of nanoparticles with cells do not change other cellular functions. An intravenous application of NPs results in a direct interaction of the nanoparticles with endothelial cells (ECs) lining the inner wall of the vasculature. It is well-known that ECs play an important role in the maintenance of the homeostasis of tissues. Therefore, the physiological function of these cells after addition of a substance into the bloodstream needs to be preserved. ER stress and UPR are factors which have been shown to impact the function of ECs in various ways (e.g. wound healing processes (Tsaryk et al. 2015). Ongoing ER stress also leads to apoptosis of cells (Szegezdi et al. 2006), and thus it is essential to minimize the effects of nanoparticles which may lead to ER stress.

Although non-toxic, the AuNPs examined in the study were internalized in varying amounts and thus one could speculate that different numbers of particles within a cell could affect the transport of proteins within the cell, resulting in a disturbance of normal cell functions and of protein transport in general. Relevant experiments showed an induction of proinflammatory cytokines and a decrease in the expression

of tight junction proteins with certain AuNPs on the brain endothelial cells. Thus, a slight modification of a NP can induce certain physiological changes in certain cells. ER stress responses as factors responsible for these phenomena were examined in detail in these studies.

No cytotoxic effect of the AuNPs was observed on hCMEC/D3 after exposure times for up to 72 hours. These results agree with those observed for primary human dermal microvascular endothelial cells (HDMEC) previously described (Freese et al. 2012a). In addition, a similar pattern of internalization of AuNPs was observed for the brain endothelial cells as for the HDMEC. However, a significant difference was observed in the uptake of 35 nm hydroxypropylamine-coated AuNPs in HDMEC and hCMEC/D3 (Freese et al. 2013). In the present study, it was shown that hCMEC/D3 internalized the surface-modified AuNPs in various amounts. Our results agree with previous studies that have shown that PEGylated AuNPs were modestly internalized in various cell types, e.g. (Bouzas et al. 2014). Our microscopic studies confirmed that the internalized AuNPs were localized in the perinuclear region of the cells and were located in vesicles as typical for these sizes of nanoparticles, and that the nanoparticles were not freely distributed in the cytoplasm (Chou, Leo Y T et al. 2011). Changes to the induction of proinflammatory mediators by the endothelial cells were examined after exposure to the various AuNPs. Although Zhang and co-workers showed that 60 nm AuNPs did not cause the induction of proinflammatory mediators (IL-6, TNF-α) in macrophages (Zhang et al. 2010), the ELISA results presented in the present study demonstrated an induction of proinflammatory mediators in hCMEC/D3. In addition, differences in the induction pattern of proinflammatory mediators were observed and these were dependent on the coating of the AuNPs. Cells exposed to glucosamine-coated nanoparticles were specially

affected, as seen by induction of the secretion of IL-8, MCP-1, soluble (s)ICAM and sVCAM. These factors are known to be induced in endothelial cells in the presence of endotoxins or TNFα (Makó et al. 2010; Buttenschoen et al. 2010; Peters et al. 2003). The AuNPs were shown to be free of endotoxin (data not shown) (Unger et al. 2014), therefore, it appears that the induction of proinflammatory mediators is a characteristic factor of the coated AuNPs. While the induction of inflammatory cytokines was shown for the medium-sized hydroxypropylamine-coated AuNPs (65-hyd), the effects induced by the glucosamine-coated AuNPs were not related to a particular size of the AuNPs. Considering the fact that various amounts of glucosamine-coated AuNPs of different sizes were internalized in hCMEC/D3, the induction of proinflammatory factors could not be attributed to the amount of nanoparticles taken up. Others have demonstrated that glucosamine itself can induce oxidative stress in primary human chondrocytes (Valvason et al. 2008), which thus might lead to the induction of inflammatory processes in endothelial cells. In contrast, other groups have shown that a direct effect of glucosamine on cells acted in an anti-inflammatory manner (Shea 2001). Nevertheless, in combination with AuNPs the induction of proinflammatory factors was significant compared to the untreated control.

A unique characteristic of brain microvascular endothelial cells is the high expression of tight junction proteins. Brain endothelial cells are highly specialized endothelial cells that form the blood-brain barrier, which is a highly organized and regulated barrier preventing the paracellular transport of most substances from the blood to the brain and vice versa. Due to differences in the uptake amounts of the various AuNPs and the expression of proinflammatory mediators, the brain endothelial cells were examined for changes in the expression pattern of tight junction proteins after

exposure to the AuNPs. Trickler et al. demonstrated a mild change in the barrier function of porcine brain endothelial cells after exposure to several sizes of unmodified AuNPs (Trickler et al. 2011). The same was shown in a previous published study that focussed on the investigation of the transport properties of hydroxypropylamine-coated AuNPs across a BBB model system (Freese et al. 2013). The decrease in the expression of tight junction proteins in hCMEC/D3 in the present study may be correlated with the induction of ER stress. Adachi et al. showed that primary human retinal endothelial cells exhibited a decreased expression of tight junction proteins as a consequence of increased ER stress (Adachi et al. 2012). Furthermore, they demonstrated that the reduction in the expression of tight junction proteins but also inflammation processes were linked to both oxidative stress and to ER stress. Changes in ER stress factors in hCMEC/D3 were evaluated in the present study and the results indicated that prominent markers of ER stress such as BiP, ATF4 and ATF6 were not differentially expressed in brain endothelial cells after exposure to the polymer-modified AuNPs. This is in contrast to Tsai et al. who demonstrated an induction of ER stress mediators followed by cytotoxicity of AuNPs in leukemia K562 cells (Tsai et al. 2011). The only factor affected in hCMEC/D3 was IRE1α. IRE1α represents one of three prominent transmembrane receptors of UPR. In addition to IRE1α upregulation the ER stress mediators, BiP and ATF6 are upregulated in activated UPR (Shen et al. 2004). However, in our study none of the mediators were affected. In addition, splicing of XBP1 mRNA was not detected. This transcription factor has been shown to be one of the most prominent markers and mediators for activated UPR. This is in accordance with the result published by Khan and colleagues, who showed that 18 nm citrate-stabilized AuNPs did not induce the splicing of XBP-1 mRNA in HeLa

cells (Khan et al. 2007). However, they did not systematically screen different sizes and surface modifications of AuNPs. Moreover, their study of ER stress was limited to the analysis of XBP1 splicing. Certainly, in combination with our studies in which all three prominent pathways of UPR were analyzed, it appears that an activation of UPR after exposure to this size of particles in different cell types can be excluded.

Various polymer-modified AuNPs were analyzed by Hauck and colleagues for potential changes in the gene expression of HeLa cells with the focus on heat shock proteins (cell stress mediators). These studies used an expression array to determine the modulation of 10,000 genes after exposure of cells to polymer-modified gold nanorods (Hauck et al. 2008). Surprisingly, only 35 genes were regulated after exposure to the gold nanorods. Most of the genes were involved in apoptosis or cell metabolic functions, but not cell stress factors. A comparison with our study is difficult on account of the different polymers used, the different shapes of the nanoparticles and the cancer cell line used by Hauck et al. Nevertheless, both studies demonstrate that cell stress mediators were not activated after treatment with polymer-coated AuNPs. Christen and colleagues focused their attention on the induction of ER stress in the human hepatoma cell line Huh7 after treatment with silica nanoparticles (SiNPs). They demonstrated an up-regulation of BiP and described splicing of XBP1 in these cells. Moreover, they showed that silver-coated SiNPs (SiO2–Ag-NPs) also induced BiP upregulation (Christen und Fent 2012). An activation of UPR in primary endothelial cells (HUVEC) and Chinese hamster ovary (CHO) cells after treatment with ZnO nanoparticles was also demonstrated by Chen and colleagues (Chen et al. 2014). However, the same study showed that CeO2 nanoparticles did not activate UPR. This was also true for the treatment of brain endothelial cells with polymer-coated AuNPs utilized in our study. In summary, these

studies demonstrate that depending on nanoparticle and cell type a range of effects on ER stress factor expression may be observed and therefore ER stress may act as a potential risk factor after NP exposure.

A final consequence of ER stress can be identified by the expression of the transcription factor CHOP and the induction of apoptosis. An analysis of CHOP expression in brain endothelial cells exposed to the different AuNPs demonstrated that apoptosis was not induced. Since ATF4, which is thought to be a dominant inducer of CHOP, was not upregulated the results in our studies are in agreement with those previously described (Harding et al. 2000). However, Tsai and colleagues showed a time-depending up-regulation of CHOP after exposure to non-coated AuNPs in leukemia cells, this being accompanied by a very rapid increase in caspase 3 expression (Tsai et al. 2011). However, both genes were again down-regulated after at least 48 hours following exposure. An induction of CHOP expression was also observed by Chen et al. in HUVEC and CHO cells after exposure to ZnO nanoparticles (Chen et al. 2014). Thus, under certain conditions and with certain NPs, the detection of ER stress-related proteins may be useful for identifying early cellular responses to nanoparticle exposure. However, our study demonstrated that polymer-modified AuNPs did not induce ER stress in brain microvascular endothelial cells.

Conclusion

We investigated the effects of twelve different gold nanoparticles on human brain endothelial cells after four different incubation times. Although different amounts of gold nanoparticles were internalized by the endothelial cells the results of the present study indicated that none of the gold nanoparticles exhibited cytotoxic effects

or induced ER stress. Furthermore, high doses of AuNPs did not induce ER stress or apoptosis even after an exposure time of 72 hours. In conclusion, none of the twelve unique polymer-modified gold nanoparticles induced ER stress factors in brain microvascular endothelial cells, although an effect on the expression of tight junction proteins could not be excluded.

Acknowledgements

This study was funded by the FP6 project 'NanoBioPharmaceutics' (NMP4-CT-2006-026723). Equipment used was supported by the Innovative Uses for Advanced Materials in the Modern World (AM2) with support from Advantage West Midlands (AWM) and partly funded by the European Regional Development Fund (ERDF).

Declaration of Interest

The authors declare that they have no competing interests.

Literaturverzeichnis

Adachi, Tetsuo; Teramachi, Mayumi; Yasuda, Hiroyuki; Kamiya, Tetsuro; Hara, Hirokazu (2012): Contribution of p38 MAPK, NF-κB and glucocorticoid signaling pathways to ER stress-induced increase in retinal endothelial permeability. In: *Archives of biochemistry and biophysics* 520 (1), S. 30–35. DOI: 10.1016/j.abb.2012.01.014.

Alkilany A. M.; Pratik K. Nagaria; Cole R. Hexel; Timothy J. Shaw; Catherine J. Murphy; Michael D. Wyatt (2009): Cellular Uptake and Cytotoxicity of Gold Nanorods: Molecular Origin of Cytotoxicity and Surface Effects. In: *Small* 5 (6), S. 701–708. DOI: 10.1002/smll.200801546.

Boisselier, Elodie; Astruc, Didier (2009): Gold nanoparticles in nanomedicine: preparation, imaging, diagnostics, therapies and toxitiy. In: *Chem. Soc. Rev* (38), S. 1759–1782. DOI: 10.1039/b806051g.

Bouzas, Virginia; Haller, Thomas; Hobi, Nina; Felder, Edward; Pastoriza-Santos, Isabel; Pérez-Gil, Jesús (2014): Nontoxic impact of PEG-coated gold nanospheres

on functional pulmonary surfactant-secreting alveolar type II cells. In: *Nanotoxicology* 8 (8), S. 813–823. DOI: 10.3109/17435390.2013.829878.

Buttenschoen, Klaus; Radermacher, Peter; Bracht, Hendrik (2010): Endotoxin elimination in sepsis: physiology and therapeutic application. In: *Langenbeck's Archives of Surgery* 395 (6), S. 597–605.

Chen, Rui; Huo, Lingling; Shi, Xiaofei; Bai, Ru; Zhang, Zhenjiang; Zhao, Yuliang et al. (2014): Endoplasmic reticulum stress induced by zinc oxide nanoparticles is an earlier biomarker for nanotoxicological evaluation. In: *ACS Nano* 8 (3), S. 2562–2574. DOI: 10.1021/nn406184r.

Chou, Leo Y T; Ming, Kevin; Chan, Warren C W (2011): Strategies for the intracellular delivery of nanoparticles. In: *Chemical Society reviews* 40 (1), S. 233–245. DOI: 10.1039/c0cs00003e.

Christen, Verena; Fent, Karl (2012): Silica nanoparticles and silver-doped silica nanoparticles induce endoplasmatic reticulum stress response and alter cytochrome P4501A activity. In: *Chemosphere* 87 (4), S. 423–434. DOI: 10.1016/j.chemosphere.2011.12.046.

Connor, E. E.; Judith Mwamuka; Anand Gole; Catherine J. Murphy; Michael D. Wyatt (2005): Gold Nanoparticles Are Taken Up by Human Cells but Do Not Cause Acute Cytotoxicity13. In: *Small* 1 (3), S. 325–327. DOI: 10.1002/smll.200400093.

Fonseca, Ana Catarina R G; Ferreiro, Elisabete; Oliveira, Catarina R.; Cardoso, Sandra M.; Pereira, Cláudia F. (2013): Activation of the endoplasmic reticulum stress response by the amyloid-beta 1-40 peptide in brain endothelial cells. In: *Biochimica et biophysica acta* 1832 (12), S. 2191–2203. DOI: 10.1016/j.bbadis.2013.08.007.

Freese, Christian; Gibson, Matthew I.; Klok, Harm-Anton; Unger, Ronald E.; Kirkpatrick, C. James (2012a): Size- and Coating-Dependent Uptake of Polymer-Coated Gold Nanoparticles in Primary Human Dermal Microvascular Endothelial Cells. In: *Biomacromolecules* 13 (5), S. 1533–1543. DOI: 10.1021/bm300248u.

Freese, Christian; Uboldi, Chiara; Gibson, Matthew I.; Unger, Ronald E.; Weksler, Babette B.; Romero, Ignacio A. et al. (2012b): Uptake and cytotoxicity of citrate-coated gold nanospheres: Comparative studies on human endothelial and epithelial cells. In: *Part Fibre Toxicol* 9 (1), S. 23. DOI: 10.1186/1743-8977-9-23.

Freese, Christian; Unger, Ronald E.; Deller, Robert C.; Gibson, Matthew I.; Brochhausen, Christoph; Klok, Harm-Anton; Kirkpatrick, C. James (2013): Uptake of poly(2-hydroxypropylmethacrylamide)-coated gold nanoparticles in microvascular endothelial cells and transport across the blood-brain barrier. In: *Biomater. Sci.* (1), S. 824–833. DOI: 10.1039/C3BM60050E.

Gibson, Matthew I.; Danial, Maarten; Klok, Harm-Anton (2011): Sequentially Modified, Polymer-Stabilized Gold Nanoparticle Libraries: Convergent Synthesis and Aggregation Behavior. In: *ACS Combinatorial Science* (13), S. 286–297.

Gibson, Matthew I.; Fröhlich, Eleonore; Klok, Harm-Anton (2009): Postpolymerization modification of poly(pentafluorophenyl methacrylate): Synthesis of a diverse water-soluble polymer library. In: *J. Polym. Sci. A Polym. Chem.* 47 (17), S. 4332–4345. DOI: 10.1002/pola.23486.

Harding, H. P.; Zhang, Y; Bertolotti, A.; Zeng, H.; Ron, D. (2000): Perk is essential for translational regulation and cell survival during the unfolded protein response. In: *Molecular cell* 5 (5), S. 897–904.

Hauck, Tanya S.; Ghazani, Arezou A.; Chan, Warren C. W. (2008): Assessing the effect of surface chemistry on gold nanorod uptake, toxicity, and gene expression in mammalian cells. In: *Small* 4 (1), S. 153–159. DOI: 10.1002/smll.200700217.

Khan, Jameel Ahmad; Pillai, Beena; Das, Taposh Kumar; Singh, Yogendra; Maiti, Souvik (2007): Molecular effects of uptake of gold nanoparticles in HeLa cells. In: *Chembiochem* 8 (11), S. 1237–1240. DOI: 10.1002/cbic.200700165.

Li, Xuemei; Zhang, Kezhong; Li, Zihai (2011): Unfolded protein response in cancer: the Physician's perspective. In: *J Hematol Oncol* 4 (1), S. 8. DOI: 10.1186/1756-8722-4-8.

Lin, Jonathan H.; Walter, Peter; Yen, T.S Benedict (2008): Endoplasmic Reticulum Stress in Disease Pathogenesis. In: *Annu. Rev. Pathol. Mech. Dis.* 3 (1), S. 399–425. DOI: 10.1146/annurev.pathmechdis.3.121806.151434.

Makó, Veronika; Czúcz, Judit; Weiszhár, Zsóka; Herczenik, Eszter; Matkó, János; Prohászka, Zoltán; Cervenak, László (2010): Proinflammatory activation pattern of human umbilical vein endothelial cells induced by IL-1β, TNF-α, and LPS. In: *Cytometry* 77A (10), S. 962–970.

Pan, Yan; Sabine Neuss; Annika Leifert; Monika Fischler; Fei Wen; Ulrich Simon et al. (2007): Size-Dependent Cytotoxicity of Gold Nanoparticles. In: *Small* 3 (11), S. 1941–1949. DOI: 10.1002/smll.200700378.

Peters, Kirsten; Unger, Ronald E; Brunner, Joachim; Kirkpatrick, C James (2003): Molecular basis of endothelial dysfunction in sepsis. In: *Cardiovascular Research* 60 (1), S. 49–57.

Phillips, Daniel J.; Prokes, Ivan; Davies, Gemma-Louise; Gibson, Matthew I. (2014): Isothermally-Responsive Polymers Triggered by Selective Binding of Fe 3+ to Siderophoric Catechol End-Groups. In: *ACS Macro Lett.* 3 (12), S. 1225–1229. DOI: 10.1021/mz500686w.

Reinhardt, Sven; Schuck, Florian; Grösgen, Sven; Riemenschneider, Matthias; Hartmann, Tobias; Postina, Rolf et al. (2014): Unfolded protein response signaling by transcription factor XBP-1 regulates ADAM10 and is affected in Alzheimer's disease. In: *FASEB journal : official publication of the Federation of American Societies for Experimental Biology* 28 (2), S. 978–997. DOI: 10.1096/fj.13-234864.

Ron, David; Walter, Peter (2007): Signal integration in the endoplasmic reticulum unfolded protein response. In: *Nature reviews. Molecular cell biology* 8 (7), S. 519–529. DOI: 10.1038/nrm2199.

Roussel, Benoit D.; Kruppa, Antonina J.; Miranda, Elena; Crowther, Damian C.; Lomas, David A.; Marciniak, Stefan J. (2013): Endoplasmic reticulum dysfunction in neurological disease. In: *The Lancet Neurology* 12 (1), S. 105–118. DOI: 10.1016/S1474-4422(12)70238-7.

Schröder, Martin; Kaufman, Randal J. (2005): The mammalian unfolded protein response. In: *Annual review of biochemistry* 74, S. 739–789. DOI: 10.1146/annurev.biochem.73.011303.074134.

Shang, Jie (2005): Quantitative measurement of events in the mammalian unfolded protein response. In: *Methods (San Diego, Calif.)* 35 (4), S. 390–394. DOI: 10.1016/j.ymeth.2004.10.012.

Shea, B. (2001): Review: glucosamine is more effective than selected non-steroidal anti-inflammatory drugs and placebo for reducing pain and more effective than placebo for improving function in patients with osteoarthritis. In: *Evidence Based Nursing* 4 (4), S. 121. DOI: 10.1136/ebn.4.4.121.

Shen, Xiaohua; Zhang, Kezhong; Kaufman, Randal J. (2004): The unfolded protein response--a stress signaling pathway of the endoplasmic reticulum. In: *Journal of chemical neuroanatomy* 28 (1-2), S. 79–92. DOI: 10.1016/j.jchemneu.2004.02.006.

Shrivastava, Rupal; Kushwaha, Pramod; Bhutia, Yang Chen; Flora, Sjs (2014): Oxidative stress induced following exposure to silver and gold nanoparticles in mice. In: *Toxicology and industrial health. DOI:* 10.1177/0748233714562623.

Szegezdi, Eva; Logue, Susan E.; Gorman, Adrienne M.; Samali, Afshin (2006): Mediators of endoplasmic reticulum stress-induced apoptosis. In: *EMBO reports* 7 (9), S. 880–885. DOI: 10.1038/sj.embor.7400779.

Tabas, Ira; Ron, David (2011): Integrating the mechanisms of apoptosis induced by endoplasmic reticulum stress. In: *Nat Cell Biol* 13 (3), S. 184–190.

Trickler, William J.; Lantz, Susan M.; Murdock, Richard C.; Schrand, Amanda M.; Robinson, Bonnie L.; Newport, Glenn D. et al. (2011): Brain microvessel endothelial cells responses to gold nanoparticles: In vitro pro-inflammatory mediators and permeability. In: *Nanotoxicology* 5 (4), S. 479–492. DOI: 10.3109/17435390.2010.540356.

Tsai, Yen-Yin; Huang, Yi-Huei; Chao, Ya-Li; Hu, Kuang-Yu; Chin, Li-Te; Chou, Shiu-Huey et al. (2011): Identification of the nanogold particle-induced endoplasmic reticulum stress by omic techniques and systems biology analysis. In: *ACS Nano* 5 (12), S. 9354–9369. DOI: 10.1021/nn2027775.

Tsaryk, R.; Bartholomä, N. M.; Simiantonaki, N.; Anspach, L.; Peters, K.; Heilmann, C. et al. (2015): ER-resident chaperones modulate inflammatory and angiogenic response of endothelial cells. In: *The British journal of dermatology. DOI:* 10.1111/bjd.13816.

Uboldi, Chiara; Bonacchi, Daniele; Lorenzi, Giada; Hermanns, M Iris; Pohl, Christine; Baldi, Giovanni et al. (2009): Gold nanoparticles induce cytotoxicity in the alveolar type-II cell lines A549 and NCIH441. In: *Particle and fibre toxicology* 6, S. 18. DOI: 10.1186/1743-8977-6-18.

Unger, Ronald E.; Peters, Kirsten; Sartoris, Anne; Freese, Christian; Kirkpatrick, C. James (2014): Human endothelial cell-based assay for endotoxin as sensitive as the conventional Limulus Amebocyte Lysate assay. In: *Biomaterials* 35 (10), S. 3180–3187. DOI: 10.1016/j.biomaterials.2013.12.059.

Valvason, C.; Musacchio, E.; Pozzuoli, A.; Ramonda, R.; Aldegheri, R.; Punzi, L. (2008): Influence of glucosamine sulphate on oxidative stress in human osteoarthritic chondrocytes: effects on HO-1, p22Phox and iNOS expression. In: *Rheumatology* 47 (1), S. 31–35. DOI: 10.1093/rheumatology/kem289.

Villiers, Christian; Freitas, Heidi; Couderc, Rachel; Villiers, Marie-Bernadette; Marche, Patrice (2010): Analysis of the toxicity of gold nano particles on the immune

system: effect on dendritic cell functions. In: *Journal of nanoparticle research : an interdisciplinary forum for nanoscale science and technology* 12 (1), S. 55–60. DOI: 10.1007/s11051-009-9692-0.

Walter, P.; Ron, D. (2011): The Unfolded Protein Response: From Stress Pathway to Homeostatic Regulation. In: *Science* 334 (6059), S. 1081–1086.

Weksler, B. B.; Subileau, E. A.; Perrière, N.; Charneau, P.; Holloway, K.; Leveque, M. et al. (2005): Blood-brain barrier-specific properties of a human adult brain endothelial cell line. In: *FASEB J.* 19 (13), S. 1872–1874. DOI: 10.1096/fj.04-3458fje.

Wilkins, Laura E.; Phillips, Daniel J.; Deller, Robert C.; Davies, Gemma-Louise; Gibson, Matthew I. (2015): Synthesis and characterisation of glucose-functional glycopolymers and gold nanoparticles: study of their potential interactions with ovine red blood cells. In: *Carbohydrate Research* 405, S. 47–54. DOI: 10.1016/j.carres.2014.09.009.

Xin, Qing; Ji, Bingyuan; Cheng, Baohua; Wang, Chunmei; Liu, Haiqing; Chen, Xiaoyu et al. (2014): Endoplasmic reticulum stress in cerebral ischemia. In: *Neurochemistry international* 68, S. 18–27. DOI: 10.1016/j.neuint.2014.02.001.

Zhang, Qin; Hitchins, Victoria M.; Schrand, Amanda M.; Hussain, Saber M.; Goering, Peter L. (2010): Uptake of gold nanoparticles in murine macrophage cells without cytotoxicity or production of pro-inflammatory mediators. In: *Nanotoxicology. DOI:* 10.3109/17435390.2010.512401.

Tables with captions

Table 1: Oligonucleotides used for real-time PCR. Oligonucleotides were synthesized by Microsynth AG (www.microsynth.ch).

Primer	forward	reverse
ATF4	5'-CTGCCCGTCCCAAACCTTAC-3'	5'-CTGCTCCGCCCTCTTCTTCT-3'
ATF6	5'-CAGAACCCCAGCCACTTTCT-3'	5'-GGCTCCGGTGAAGAGAGACT-3'
BiP	5'-ACTATGAAGCCCGTCCAGAAAGT-3'	5'-TCGAGCCACCAACAAGAACA-3'
CHOP	5'-CACCACTCTTGACCCTGCTTC-3'	5'-GCTCTGGGAGGTGCTTGTGA-3'
claudin-5	5'-GCCCTTAACAGACGGAATGA-3'	5`-CTGCCGATGGAGTAAAGACC-3'
Grp94	5'-CGCTTCGGTCAGGGTATCTTT-3'	5'-CCTTTGCATCAGGGTCAATGT-3'
IRE1a	5'-CTGGAGCCTAGAGAAGCAGC-3'	5'-TTCTCATGGCTCGGAGGAGA-3'
occludin	5'-ACTTCAGGCAGCCTCGTTAC-3'	5'-CCTGATCCAGTCCTCCTCCA-3'
PERK	5'-CCTTGGTGTCATCCAGCCTT-3'	5'-ATGCTTTCACGGTCTCGGTC-3'
RPL13A	5'-CCTGGAGGAGGAGAGGAAAGAGA-3'	5'-TCCGTAGCCTCATGAGCTGTT-3'
Xbp1 spliced	5'-CAGGATTCTGGCGGATTGACTC-3‘	5'-CTGGGGAAGGGCATTTCAAGAA-3'
ZO-1	5'-TGCCATTACACGGTCCTCTG-3'	5'-GGTTCTGCCTCATCATTTCCTC-3'

Figures captions

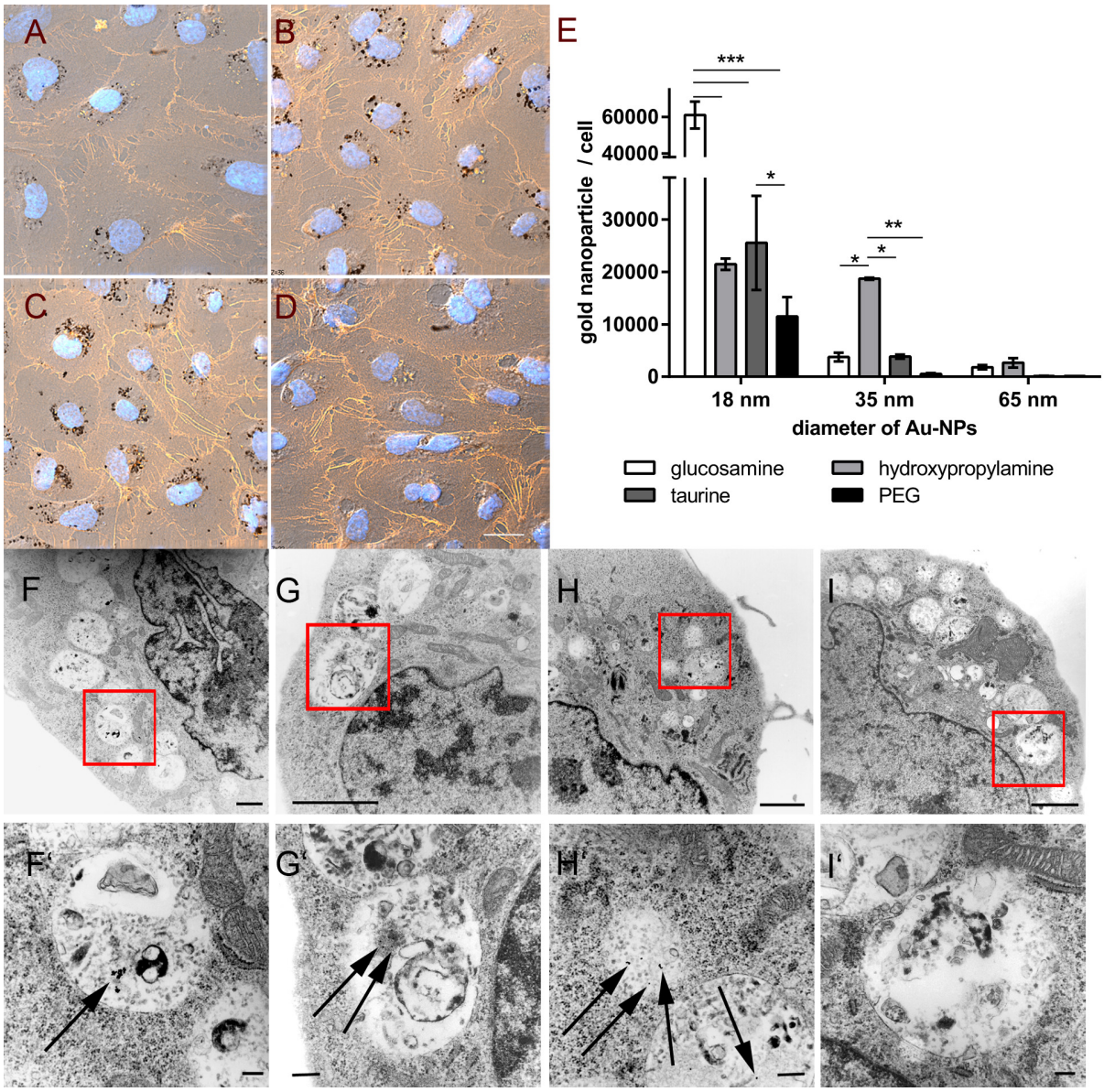

Figure 1: Uptake of various gold nanoparticles by endothelial cells after 24 hours of exposure.

hCMEC/D3 were exposed to 100 µg / mL AuNPs for 24 hours. (A - D) Cells were fixed and membranes were stained with anti-CD31 antibody (red). Nuclei were stained with Hoechst dye (blue). Agglomerates of AuNPs were detected as black dots (optical/fluorescence microscopy, Delta Vision, 60x; scale bar: 10 µm). (A) 35 nm – glucosamine; (B) 35 nm – hydroxypropylamine; (C) 35 nm – taurine; (D) 35 nm – PEG. (E) Cells exposed to various gold nanoparticles were analyzed for internalized gold nanoparticles by ICP-AES. Amounts of AuNPs were calculated per

cell. Results are shown as means ± SEM of four independent experiments each performed in triplicate (n = 4). *: P < 0.05, **: P > 0.01; ***: P < 0.001 (TWOway ANOVA with Tukey t-test). (F – I) Cells were exposed to AuNPs and analyzed by transmission electron microscopy (scale bar: 1.9 µm). Higher magnifications are shown in F' – I' (scale bar: 200 nm). (F) @glucosamine; (G) @hydroxypropylamine; (H) @taurine; (I) @PEG.

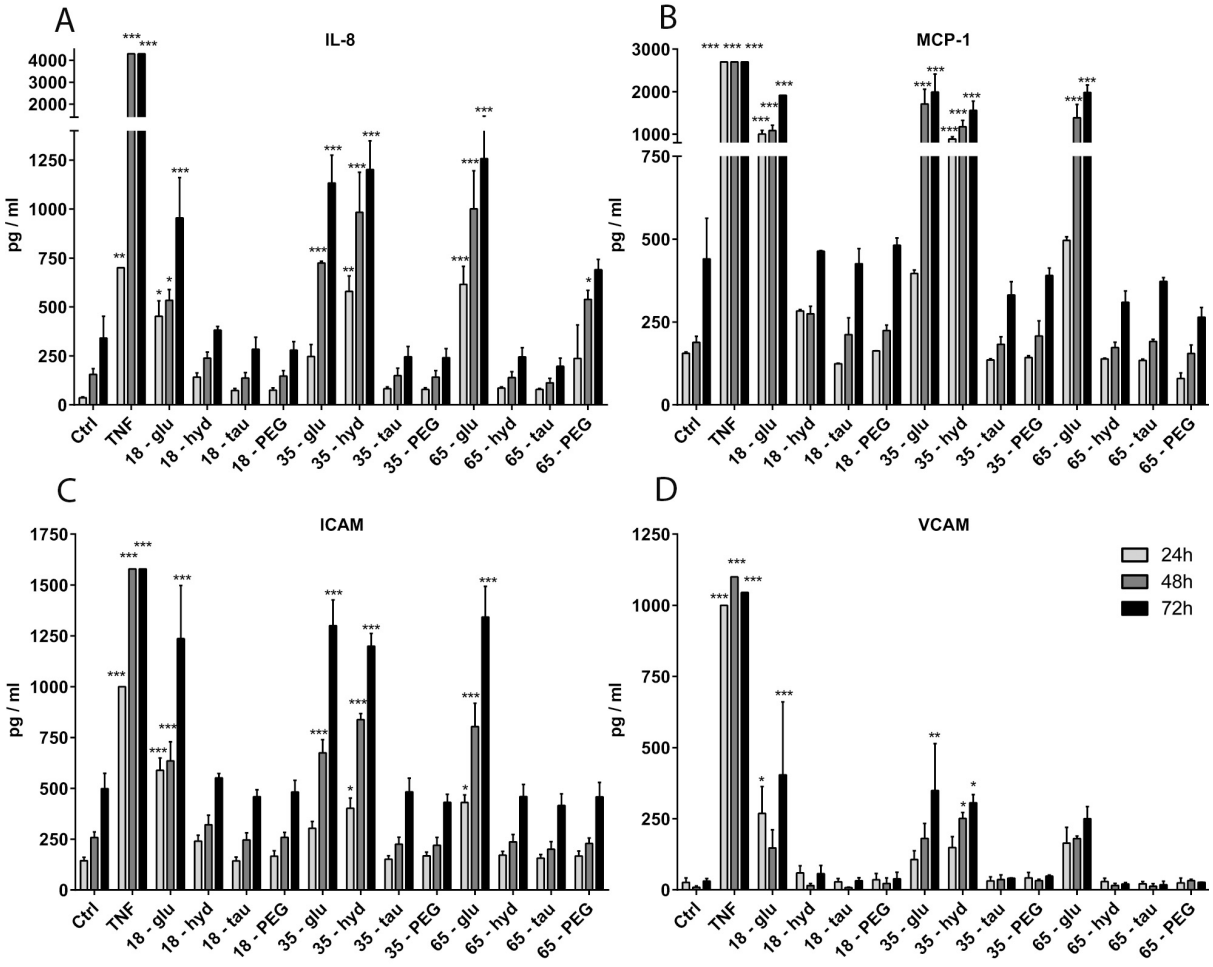

Figure 2: Cytokine secretion of hCMEC/D3 after treatment with different gold nanoparticles.

hCMEC/D3 were treated with 150 µg / mL AuNPs of different sizes and surface modifications. The concentrations of proinflammatory mediators ((A) IL-8, (B) MCP-1, (C) sICAM, (D) sVCAM) were determined using ELISA after 24h, 48h and 72h.

TNFα treated cells were used as positive control. Untreated cells were used as control (Ctrl). The data represents the means ± SEM of two independent experiments each performed in triplicate (n = 2). *: P < 0.05, **: P > 0.01; ***: P < 0.001 (TWOway ANOVA with Dunnett t-test).

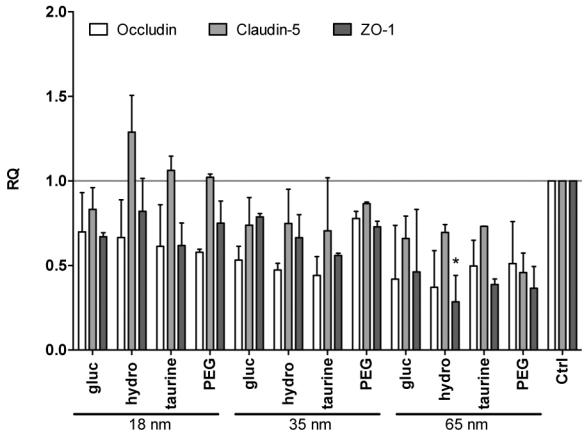

Figure 3: Expression of tight junction proteins in hCMEC/D3 after treatment with different gold nanoparticles

hCMEC/D3 were treated with 150 µg / mL gold nanoparticles of different sizes and surface modifications for 48 hours. The relative quantification of TJ proteins was determined using real-time PCR. Untreated cells have been used as control. The data represents the means ± SEM. of two independent experiments each performed in triplicate (n = 2). *: P < 0.05 (ONEway ANOVA with Dunnett t-test).

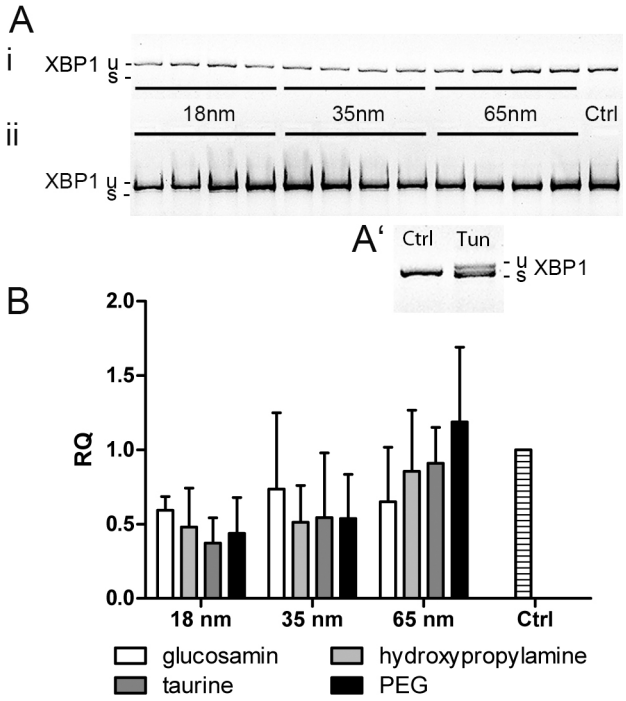

Figure 4: Impact of AuNP treatment on the splicing of transcription factor XBP1 mRNA as an indication of UPR activation.

hCMEC/D3 were treated with various AuNPs for 4 hours. Cells were analyzed for XBP1 mRNA splicing. (A) PCR was performed with XBP1 primers that amplify both variants of XBP1, unspliced (u) and spliced (s) variants. Cells treated with 10 µg / mL (i) or 150 µg / mL (ii) AuNPs were analyzed. Samples were plotted in the following order: glucosamine, hydroxypropylamine, taurine, PEG coated AuNPs. (A') Tunicamycin was used as positive control for XBP1 splicing. (B) For the same samples (150 µg / mL) the amount of spliced XBP1 was quantified using real-time PCR. Untreated cells have been used as control. The data represents the means ± SEM of two independent experiments each performed in triplicate (n = 2). (TWOway ANOVA with Dunnett t-test).

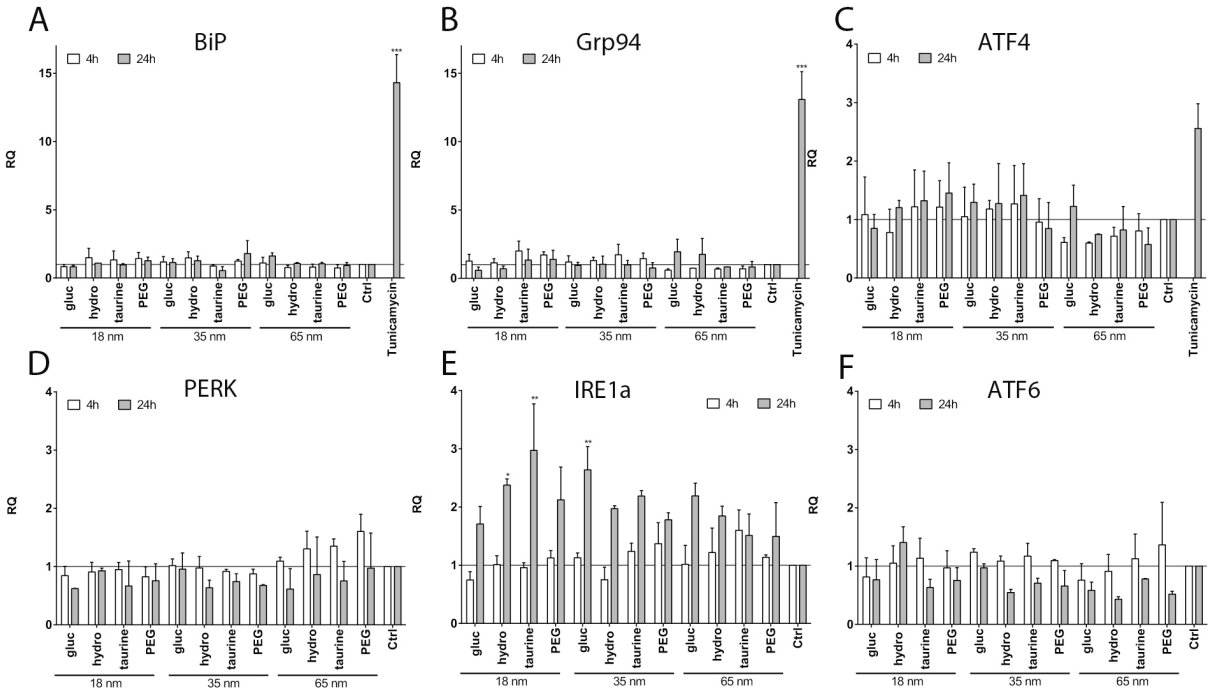

Figure 5: Expression of UPR-related genes upon exposure to AuNPs.

hCMEC/D3 were treated with various 150 µg / mL AuNPs for 4 and 24 hours. Real-time PCR was used to quantify the expression of UPR related genes: (A) BiP, (B) Grp94, (C) ATF4, (D) PERK, (E) IRE1α, (F) ATF6. The data represents the means ± SEM of two independent experiments each performed in triplicate (n = 2). *: $P < 0.05$, **: $P > 0.01$ (TWOway ANOVA with Dunnett t-test).

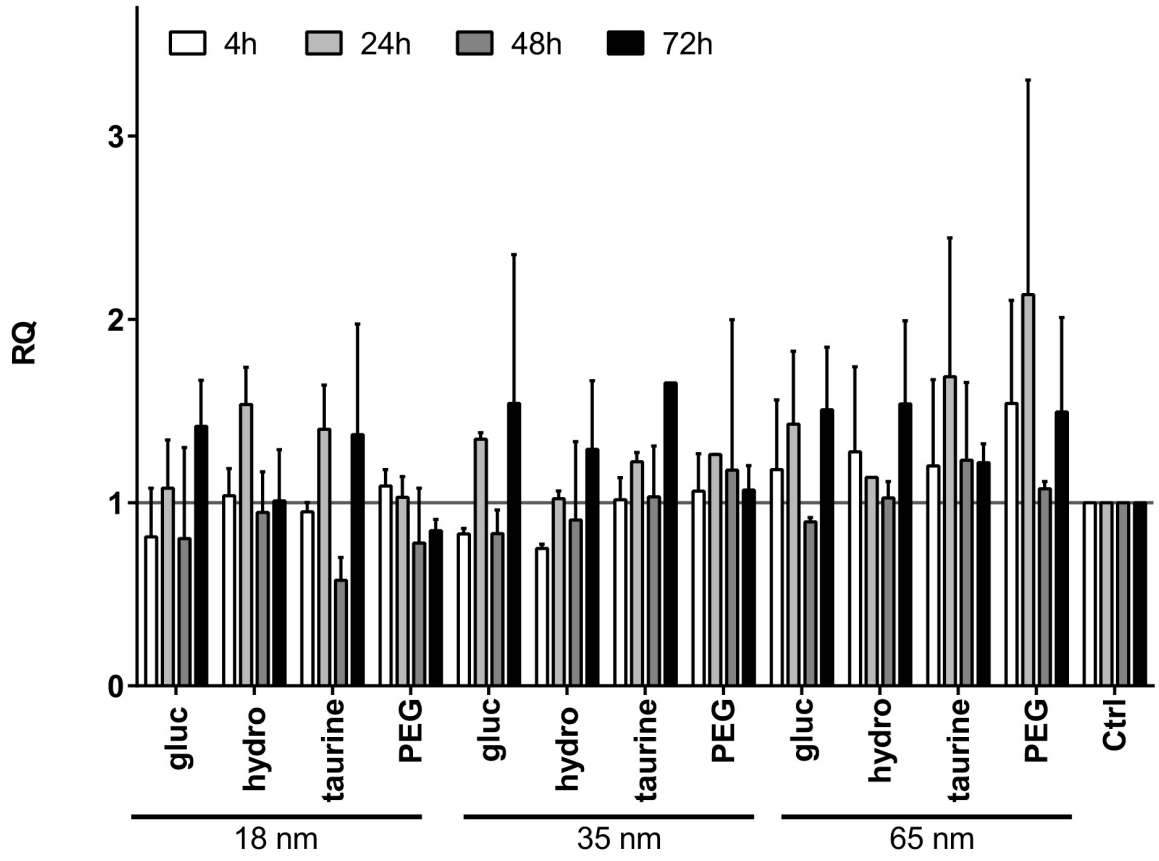

Figure 6: Expression of CHOP in brain endothelial cells after AuNP treatment.

hCMEC/D3 were treated with various 150 µg / mL AuNPs for various time points. The expression of CHOP was quantified by real-time PCR. Data are shown as relative quantification (RQ). Untreated control was set to 1. The data represents the means ± SEM of two independent experiments each performed in triplicate (n = 2). (TWOway ANOVA with Dunnett t-test).

Supplementary Material:

Impact of polymer-modified gold nanoparticles on brain endothelial cells: exclusion of endoplasmic reticulum stress as a potential risk factor.

Laura Anspach[1], Ronald E. Unger[1], Matthew I. Gibson[2], Harm-Anton Klok[3], C. James Kirkpatrick[1], Christian Freese*[1]

Address: [1]REPAIR-lab, Institute of Pathology, University Medical Center of the Johannes Gutenberg University Mainz and European Institute of Excellence on Tissue Engineering and Regenerative Medicine, Mainz, Germany; [2]University of Warwick, Department of Chemistry, Coventry, CV4 7AL, United Kingdom; [3]École Polytechnique Fédérale de Lausanne (EPFL), Institut des Matériaux and Institut des Sciences et Ingénierie Chimiques, Laboratoire des Polymères, Bâtiment MXD, Station 12, CH-1015 Lausanne, Switzerland.

*Corresponding author: Christian Freese, Langenbeckstr. 1, 55131 Mainz, Germany; Phone: +49-6131-17-3925, Email: freesec@uni-mainz.de

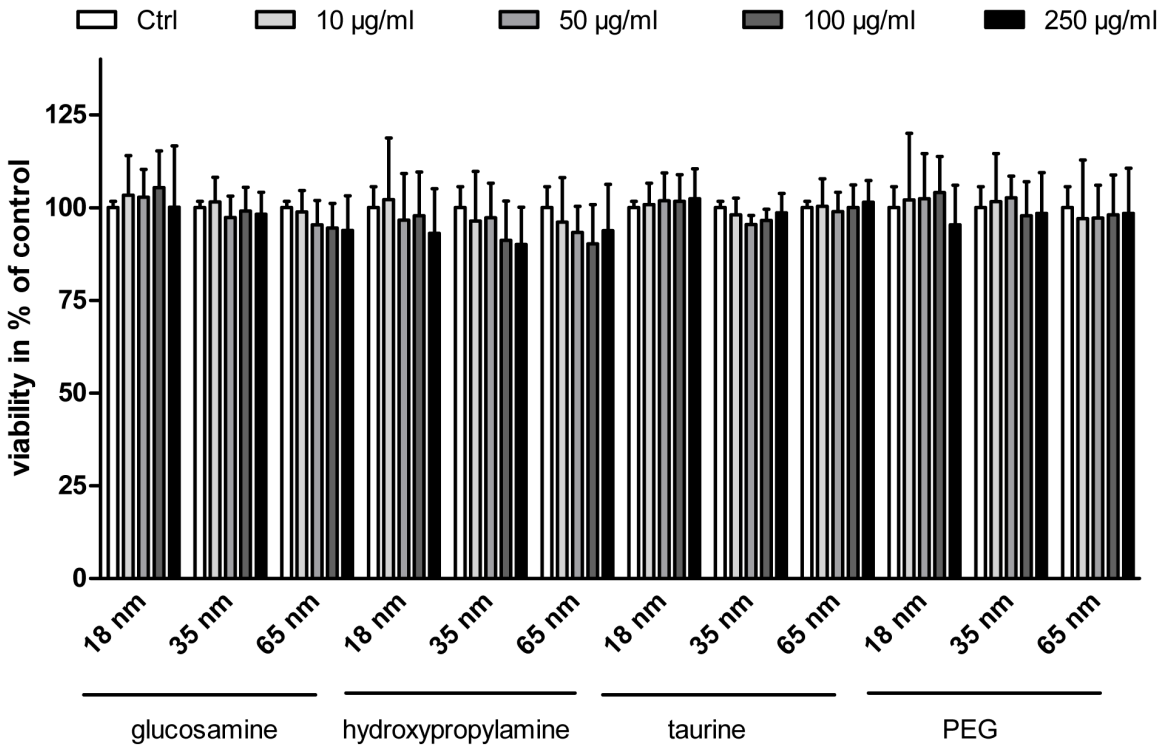

Supplementary Material Figure 1: Cell viability of hCMEC/D3 after exposure to gold nanoparticles

The endothelial cells hCMEC/D3 were exposed to different concentrations of gold nanoparticles (10, 50, 100, 250µg/ml) for 48 hours. Cell viability was measured by MTS assay. The cell viability of untreated cells (Ctrl) was set to 100%. Each column represents the mean ± standard deviation of three independent experiments; each of these was performed at least in triplicate ($n \geq 3$; (TWOway ANOVA with Tukey t-test)).

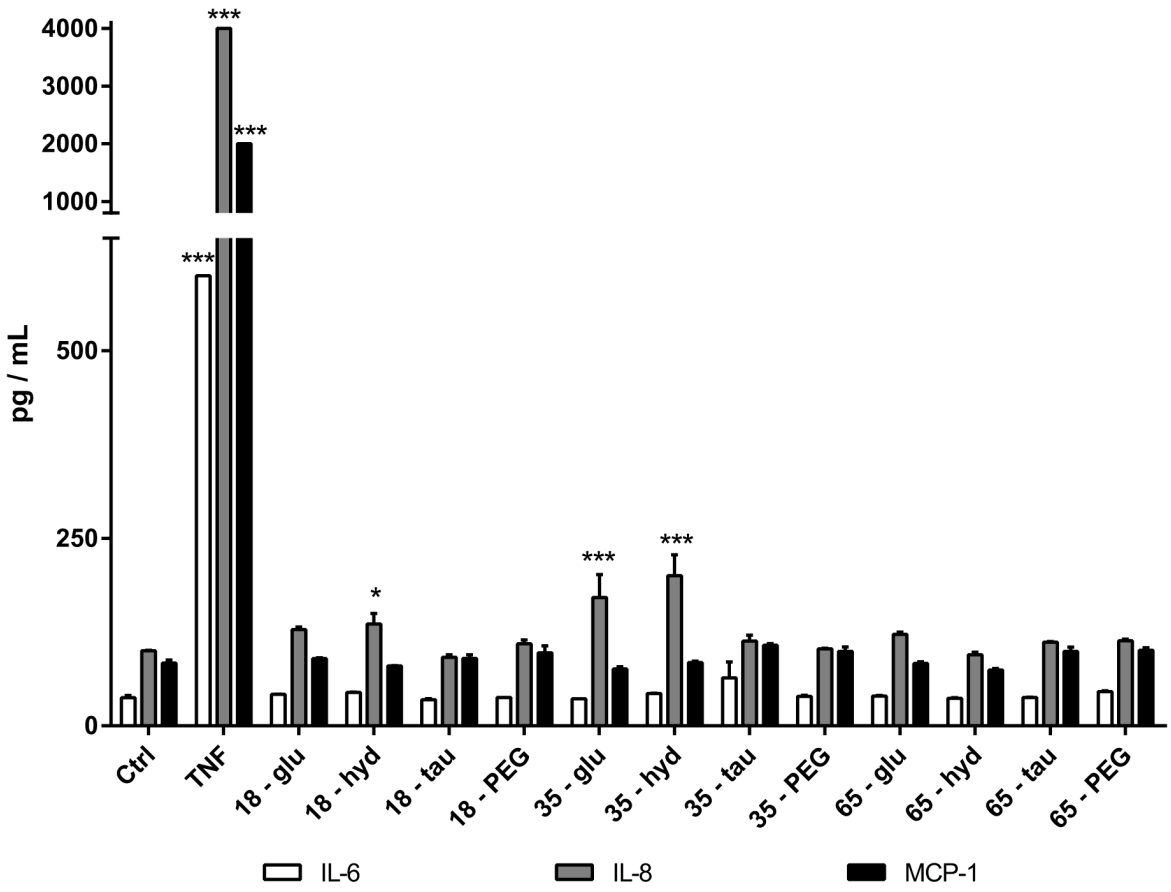

Supplementary Material Figure 2: Cytokine secretion of hCMEC/D3 after treatment with different gold nanoparticles.

hCMEC/D3 were treated with 10 µg / mL gold nanoparticles of different sizes and surface modifications. The concentrations of pro-inflammatory mediators (IL-6, IL-8 and MCP-1) were determined using ELISA after 24h. TNFα treated cells were used as positive control. Untreated cells were used as control (Ctrl). Each column represents the mean ± standard deviation. *: $P < 0.05$, ***: $P < 0.001$; ($n \geq 2$; (TWOway ANOVA with Tukey t-test)).

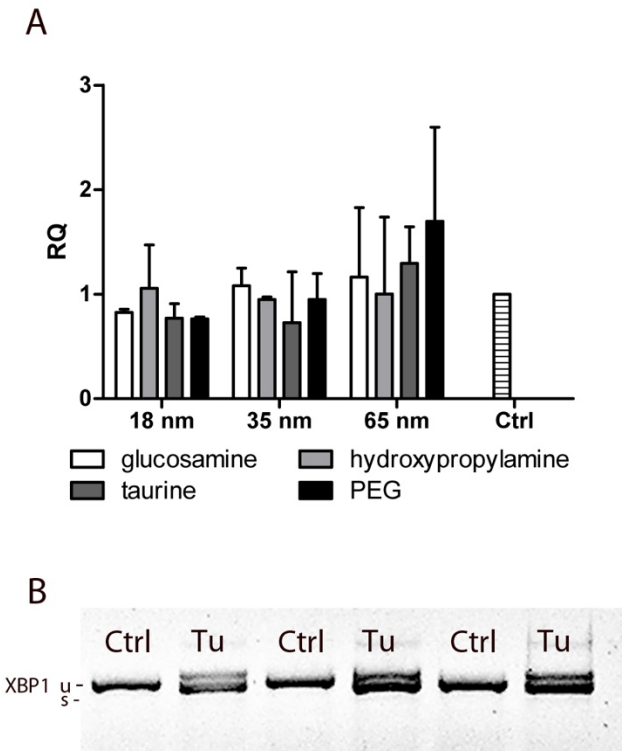

Supplementary Material Figure 3: Impact of AuNP treatment on the splicing of transcription factor XBP1 mRNA.

hCMEC/D3 were treated with various AuNPs (150 µg / mL) for 24 hours. Cells were analyzed for spliced XBP1 mRNA splicing using Real-time PCR (A), while RPL13A was detected as reference gene. Untreated control was set to 1. Each column represents the mean ± standard deviation (n = 2) (B) Cells were treated with Tunicamycin (Tu) as positive control for ER stress and XBP1 splicing for 24 hours. PCR was performed with XBP1 primers that amplify both variants of XBP1, unspliced (u) and spliced (s) variants.

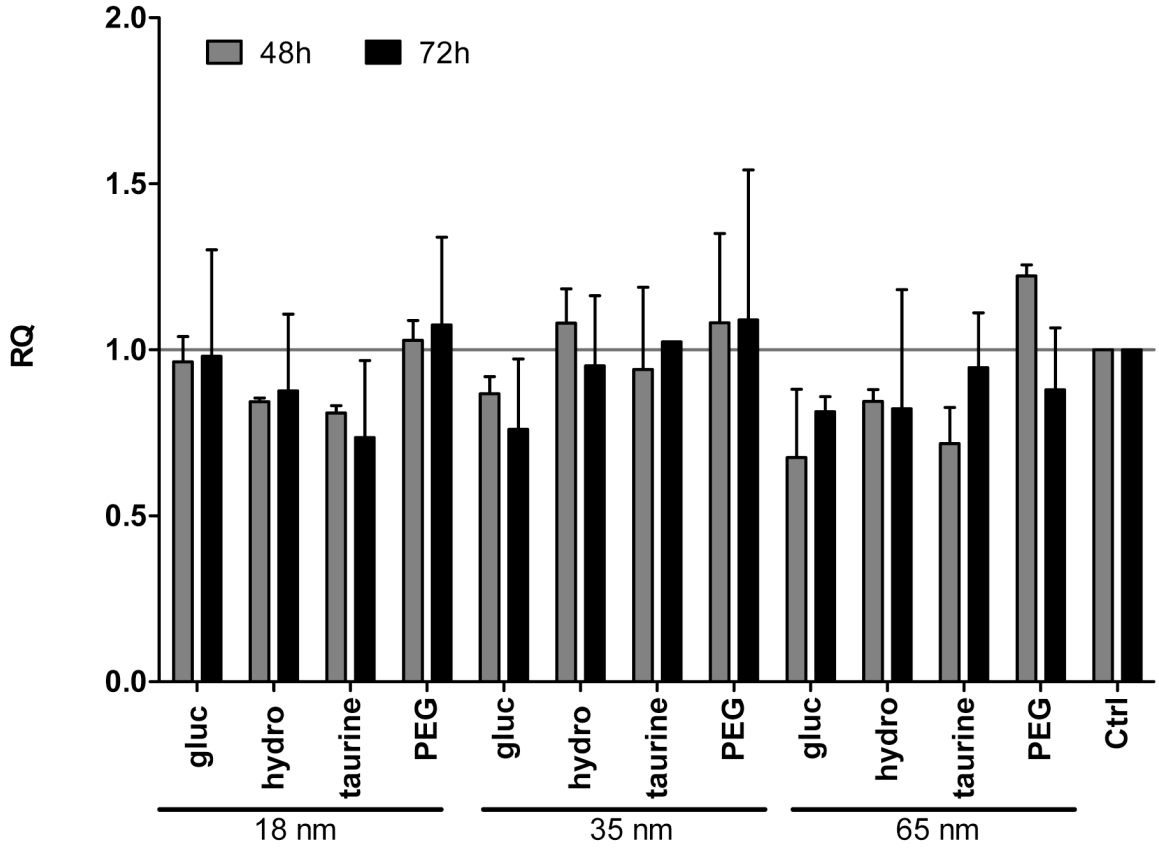

Supplementary Material Figure 4: Expression of BiP upon exposure to AuNPs

hCMEC/D3 were treated with various AuNPs (150 µg / mL) for 48 and 72 hours. Real-time PCR was used to quantify the expression of BiP. RPL13A was detected as reference gene. Data are shown as relative quantification (RQ). Untreated control was set to 1. Each column represents the mean ± standard deviation (n = 2).